Well-balanced shock-capturing hybrid finite volume - finite difference schemes for Boussinesq-type models

M. Kazolea[a], and A.I. Delis[b]
[a] Department of Environmental Engineering, Technical University of Crete, University Campus, Chania, Crete, Greece.
[b]Department of Sciences, Technical University of Crete, University Campus, Chania, Crete 73100, Greece
mskazolea@isc.tuc.gr, adelis@science.tuc.gr

Abstract. A formally forth-order, in space and time, well-balanced hybrid finite volume/ difference numerical scheme for approximating the Boussinesq-type formulations of Nwogu and Madsen and Sörensen is presented. The scheme utilizes the approximate Riemann solver of Roe for the inter-cell advective fluxes and bathymetry source term, and finite difference discretizations for the dispersive terms. Special attention is given to the numerical treatment of wet/dry fronts, friction term and wave breaking. To access the performance and expose the merits and differences of the two Boussinesq formulations the numerical model has been applied to a number of idealized and experimental test cases.

Key words: Boussinesq-type equations, finite volume method, solitary waves, run-up, breaking waves

1 Introduction

In the last two decades numerical modeling of free surface flows has been one of the most interesting fields in coastal engineering. In particular, depth averaged models have gained a lot of popularity, with the nonlinear shallow water equations (NSWE) being one of the most applied models falling in this category. However, NSWE are not appropriate for deeper waters where dispersion effects become more important than nonlinearity. On the other hand Boussinesq-type equations introduce dispersion terms and are more applicable in water where dispersion begins to have an effect on the free surface. The extended Boussinesq formulations of Madsen and Sörensen [1] and Nwogu [3] have received, probably, the most attention in recent years. In this work both formulations are solved using a Godunov-type finite volume technique, based on the approximate Riemann solver of Roe with the bathymetry source term discretized as to provide a well-balanced scheme, also in the presence of wet/dry fronts which are properly handled in the numerical model. Also two wave breaking models are presented and tested following recent advances in the field.

Nwogu [3] derived a system of equations using the water velocity u_a at an arbitrary distance, z_a, from a still water level, d, as the velocity variable, instead of the commonly used depth-averaged velocity. An optimum value of $z_a = 0.531d$ was used, so that the dispersion properties of the system most closely approximate those defined by linear

wave theory, making the equations applicable to a wider range of water depths. The equations can be reformulated in vector conservative form, [4], as

$$\mathbf{U}_t + \mathbf{F}(\mathbf{U})_x = \mathbf{S}(\mathbf{U}). \tag{1}$$

where $\mathbf{U}$ is the vector of the conserved variables, $\mathbf{F}$ is the flux vector and $\mathbf{S}$ is the source term,

$$\mathbf{U} = \begin{bmatrix} H \\ P^* \end{bmatrix}, \quad \mathbf{F}(\mathbf{U}) = \begin{bmatrix} Hu \\ Hu^2 + \frac{1}{2}gH^2 \end{bmatrix}.$$

$H = d + \eta$ is the total water depth, η the free surface elevation and $u_a \equiv u$ is the horizontal flow velocity.

$$P^* = Hu + Hz_a\left(\frac{z_a}{2}u_{xx} + (du)_{xx}\right) \tag{2}$$

is the velocity function that contains all time-derivatives in the momentum equation and a part of the dispersion terms while g is the gravitational acceleration. The source term $\mathbf{S}(\mathbf{U}) = \mathbf{S_b} + \mathbf{S_f} + \mathbf{S_d}$ models the effects of the shape of the topography, friction and a part of the dispersion terms. By denoting with b the bed topography elevation, $\mathbf{S_b} = [0, \ -gHb_x]^{\mathrm{T}}$, $\mathbf{S_f}$ includes the bed friction stresses, given as $\mathbf{S_f} = [0, \ -ghS_f]^{\mathrm{T}}$ with $S_f = \frac{n_m^2 u\|u\|}{H^{4/3}}$ and $\mathbf{S_d} = [-\psi_C, \ -u\psi_C + \psi_M - R_b]^{\mathrm{T}}$ contains the dispersion terms.

$$\psi_M = H_t z_a\left(\frac{z_a}{2}u_{xx} + (du)_{xx}\right), \quad \psi_C = \left[\left(\frac{z_a^2}{2} - \frac{d^2}{6}\right)du_{xx} + \left(z_a + \frac{d}{2}\right)d(du)_{xx}\right]_x \tag{3}$$

R_b represents the parametrization of wave-breaking characteristics.

The equations derived by Madsen aad Sörensen (MS) [1] for a slowing varying bathymetry, are written also in conservative form (1) following [2]. Now the velocity function P^* has the form:

$$P^* = Hu - (B + \frac{1}{3})d^2(Hu)_{xx} - \frac{1}{3}d_x(Hu)_x. \tag{4}$$

with $B = 1/15$ being a free parameter that determines the system's dispersion properties [1]. The source term $\mathbf{S}(\mathbf{U}) = \mathbf{S_b} + \mathbf{S_f} + \tilde{\mathbf{S}}_\mathbf{d}$, with $\mathbf{S_b}$ and $\mathbf{S_f}$ exactly as in Nowgu's equation but now $\tilde{\mathbf{S}}_\mathbf{d} = [0, \ -\psi - R_b]^{\mathrm{T}}$ where

$$\psi = -Bgd^3\eta_{xxx} - 2d^2d_xBg\eta_{xx}. \tag{5}$$

2 The numerical scheme

The numerical scheme developed to solve the two sets of equations is formally fourth order accurate in space and in time. We use the finite volume formulation for the discretization of the advective part of the equations and the bed source term and finite difference formulations for the dispersive terms. A Cartesian mesh is used in which

index i represents the centroid of a particular computational cell, C_i, where the average quantities of the conserved variables, denoted as $\mathbf{U}_i(t)$, are nominally stored. After integration of (1) over each control volume C_i the advective and the bed source terms:

$$\left[\begin{array}{c} Hu \\ Hu^2 + \frac{1}{2}gH^2 \end{array}\right]_i - \left[\begin{array}{c} 0 \\ -ghb_x \end{array}\right]_i = -\frac{1}{\Delta x}\Delta \mathbf{F}_i + \frac{1}{\Delta x}\Delta \mathbf{R}_i \tag{6}$$

where $\Delta \mathbf{F}_i$ is the flux variation from the right to the left cell and $\Delta \mathbf{R}_i$ is the contribution of the bed where up-winding of the topography source term is performed [7]. The numerical fluxes in Equation (6) can be evaluated solving the Riemann problem at the cell interfaces. In this study the approximate Riemann solver of Roe [7] is utilized. High-order accuracy in the calculation of fluxes is achieved by constructing cell interface values using a fourth order MUSCL reconstruction, prior to the application of the Riemann solver [2, 6]. This fourth order reconstruction is performed, to the total water depth H, velocity u, and bed b.

In both formulations the dispersion terms contain spatial derivatives of up to third order. According to [5] a fourth order accurate treatment of the first-order derivatives is required so that the truncation errors in the numerical scheme are smaller than the dispersion terms present in the model. We discretize them using fourth order central difference approximations for first order derivatives, third order central difference approximations for third order derivatives and second order for second order derivatives. In Nowgu's formulation in order to discretize the term ψ_C in the continuity equation, we evaluate the first and second-order derivatives of the flow velocity at the cell interfaces using Taylor series expansion as:

$$\phi_{i+1/2} = \frac{7(\phi_{i+1} + \phi_i) - (\phi_{i+2} - \phi_{i-1})}{12}, \quad (\phi_{i+1/2})_{xx} = \frac{(\phi_{i+2} + \phi_{i-1}) - (\phi_{i+1} - \phi_i)}{2\Delta x^2}$$

resulting to

$$\begin{aligned}(\psi_c)_i = \frac{1}{\Delta x}\Bigg[& \left(\left(\frac{(z_a)_{i+1/2}^2}{2} - \frac{d_{i+1/2}^2}{6}\right) d_{i+1/2}(u_{i+1/2})_{xx}\right. \\ & \left. + \left((z_a)_{i+1/2} + \frac{d_{i+1/2}}{2}\right) d_{i+1/2}(d_{i+1/2}u_{i+1/2})_{xx}\right) \\ & - \left(\left(\frac{(z_a)_{i-1/2}^2}{2} - \frac{d_{i-1/2}^2}{6}\right) d_{i-1/2}(u_{i-1/2})_{xx}\right. \\ & \left. + \left((z_a)_{i-1/2} + \frac{d_{i-1/2}}{2}\right) d_{i-1/2}(d_{i-1/2}u_{i-1/2})_{xx}\right)\Bigg].\end{aligned}$$

For the momentum disspersion term ψ_M we discretize the second order derivative using second order central difference, $u_{xx} = \frac{u_{i-1} - 2u_i + u_{i+1}}{\Delta x^2}$, hence ψ_M is then given by

$$(\psi_M)_i = (H_i)_t (z_a)_i \left(\frac{(z_a)_i}{2}(u_i)_{xx} + (h_i u_i)_{xx}\right). \tag{7}$$

The term $(H_i)_t$ can be explicitly obtain from the continuity equation in terms of spatial derivatives only.

For the MS formulation, to discretize the term ψ of the momentum equation, use:

$$(\phi_i)_x = \frac{\phi_{i-2} - 8\phi_{i-1} + 8\phi_{i+1} - \phi_{i+2}}{12\Delta x}, \quad (\phi_i)_{xxx} = \frac{\phi_{i+2} - 2\phi_{i+1} + 2\phi_{i-1} - \phi_{i-2}}{2\Delta x^3}, \quad (8)$$

and applying (8) in equation (5) results in:

$$\psi_i = -\frac{Bgd_i^3}{\Delta x^3}\left[\eta_{i+2} - 2\eta_{i+1} + 2\eta_{i-1} - \eta_{i-2}\right] - \frac{Bgd_i^2}{6\Delta x^3}\left[(d_{i-2} - 8d_{i-1} + 8d_{i+1} - d_{i+2})(\eta_{i-1} - 2\eta_i + \eta_{i+1})\right] \quad (9)$$

In order to keep the well-balanced (C-property) in the fourth order MUSCL discretization an extra term is added to the source term discretization for maintaining the correct balance [8]. In the boundary defined by a wet/dry front a special treatment is also needed. In order to identify a dry cell, a tolerance parameter is used. Reconstructed values are computed as to satisfy $\frac{\partial \eta}{\partial x} = -\frac{\partial b}{\partial x}$. Bed slope is redefined as to satisfy an extended C-property [8] and numerical fluxes at the wet/dry interface are computed assuming temporarily zero velocity. Finally the error due to possible negative depths or due to the imposed threshold are summed and added properly into the entire computational domain [8].

As proposed by Wei and Kirby [5], time integration should be fourth-order accurate since first to third order spatial derivatives are included in both formulations. Here, time integration is achieved in two stages, namely the third order Adams-Basforth predictor stage and the fourth-order Adams-Moulton corrector stage [2, 4]. The predictor and the corrector stages update the values of the velocity function P^* given by equations (2) and (4) for the respective formulations. The values of hu and therefore the velocities need to be extracted after, booth stages, by solving a tridiagonal system resulting from the discretizations of the spatial derivatives by using the finite difference method. In order to handle the friction terms a separate implicit formulation [8] was applied after the predictor and the corrector stages.

The shallow water steepness is the primary cause of breaking for waves on a beach. As the wave amplitude increases and reaches a critical level wave crest steepen, the front of the wave becomes vertical and then the crest of the wave overturns. At this point physical models like Boussinesq equations are unable to describe the physical procedure and a wave breaking model is necessary. Two wave breaking models are considered in this work. The first one is an eddy viscosity approach [4] and the second one is based in NSWE [2]. In the model proposed in [4] , an extra wave breaking term is added to the equations in order to dissipate the energy.

$$R_B = [\upsilon(Hu)_x]_x, \quad \text{with } \upsilon = -BH|Hu|_x \quad \text{and} \quad B = 1 - \frac{(Hu)_x}{U_1}. \quad (10)$$

where υ is the eddy viscosity calibrated to describe energy dissipation in breaking process. $(Hu)_x$ is used as the indicator, to determine the eddy viscosity. Using this indicator we better detect stationary or slow-moving hydraulic jumps. U_1, U_2 are the flow speeds at the onset and termination of the wave-breaking process [4].

The idea behind the approach proposed in [2] is that Boussinesq equations degenerate into NSWE as dispersive terms become negligible compared to nonlinear terms.

Hence, a criterion is introduced to determine the domain where the nonlinearity prevails and the NSWE are solved. Using the Froude number and after some computations [2] the value of $\epsilon = A/d$ is chosen to be the criterion to switch from Boussinesq equations to NSWE, where A is the wave's amplitude. Consequently in each cell we check ϵ, if $\epsilon \leq 0.8$ Boussinesq equations are solved, otherwise the dispersive terms are switched off and the NSWE are solved.

3 Numerical tests and results

We first consider the standard test of a solitary wave propagation over a flat bottom. The wave should maintain its shape, speed and amplitude as it travels, due to an exact balance between the nonlinear and dispersion terms. Two solitary waves of different amplitudes $A/d = 0.1$, $A/d = 0.3$ were considered. Their initial set-up of the problem can be found in [5] and [6]. Fig. 1 shows the surface profile for the first wave for both models. For Nwogu's formulation a slightly higher wave was formed, which propagated

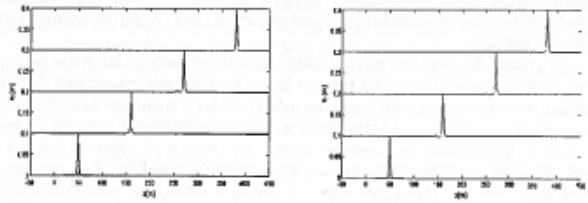

Fig. 1. Water surface profile of the solitary wave ($A/d = 0.1$) propagating down a channel at times $t = 0, 50, 100, 150$s for Nwogu's (left) and Madsen and Sörensen's (right) formulation.

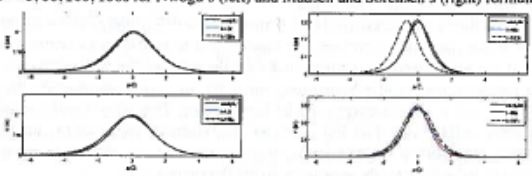

Fig. 2. Comparison of the solitary wave $A/d = 0.1$ (left) and $A/d = 0.3$ (right) shape at $t = 40$s and $t = 160$s, for Nwogu's (up) and Madsen and Sörensen's (down) formulation.

with a constant shape and amplitude. For the MS formulation a train of small waves was formed which is soon left behind and the wave changes shape becoming wider and less tall but after some time the wave's shape was stabilized and reached a numerical permanent form. A comparison of the normalized numerical and analytical wave solutions is given in Fig. 2.

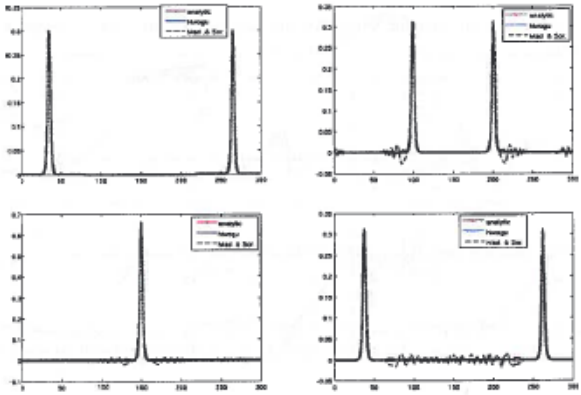

Fig. 3. Head-on collision of two solitary waves

The second case is the counter-propagation of two symmetric solitary waves. Two solitary waves with an equal initial hight of $A/d = 0.3$ are placed in positions $x/d = 35$ and $x/d = 265$. The initial wave surface elevation and velocity can be found in [5] for Nwogu's equations and in [2] for the MS formulation. $\Delta x/d = 0.1$. $d = 1.0$ and $CFL = 0.2$. Fig. 3 shows the surface profiles at times $t\sqrt{g/d} = 0, 56.63, 101.2. 200$. The initial waves undergoes an evolution and two slightly higher solitary waves are formed, which propagate with a constant amplitude $A/d = 0.3135$ until the collision. At time $t\sqrt{g/d} = 101.2$ the wave gets its highest pick $A/d = 0.66$ for Nwogu's formulation and $A/d = 0.59$ for that for MS one. After the collision the numerical solution has a small phase sift compared to the analytic one. We note that after the head-on collision of the waves small amplitude dispersive tails were developed. The dispersive tails are more intense for the MS model due to the discrepancy between the analytical solution given as input to the model.

The next problem presented here compares numerical and experimental results of the runup, rundown and wave breaking of a solitary wave on a plane beach. Synolakis (see [7] for details) presented a series of surface profiles from his runup experiments for a beach of slope $1 : 19.85$ with $A/d = 0.28$ initially. The wave broke strongly during both the runup and the rundown. We used $CFL = 0.4$ and $\Delta x = 0.2$. while Breaking model (10) was applied for both Boussinesq models. Fig. 4 presents the series of the surface profile for Nwogu's, Madsen and Sörensen's and the NSWE. Both Boussinesq models reproduce the shoaling process up to $t\sqrt{g/H} = 20$ against the NSWE which don't include dispersive terms to balance the nonlinear effects. The models showed a minor discrepancy with the experimental data at $t\sqrt{g/H} = 45$ when a hydraulic jump

begins to develop from the drowdown but computed results fully recovered in later times.

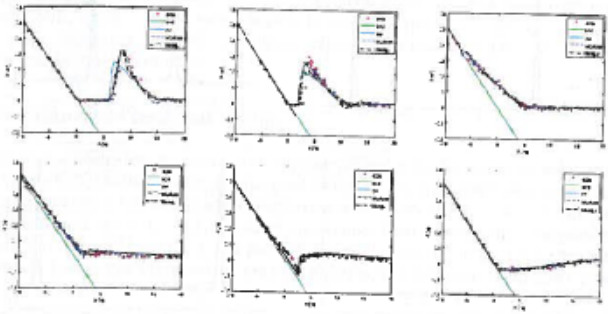

Fig. 4. Solitary wave runup on a plane beach, $A/d = 0.28$, at $t\sqrt{g/H} = 15, 20, 30, 45, 60, 80$.

The final two experimental test cases, presented in [4], are on solitary wave transformation over idealized fringing reefs (the second case includes a fore reef slope) and examine the model's capability in handling nonlinear dispersive waves together with wave breaking and bore propagation. For both tests Tonneli's breaking model was used for the MS equations and breaking model (10) for Nowgu's equations. The first case involves a steep solitary wave of $A/d = 0.5$ and the second one a wave of $A/d = 0.3$. In the first case the wave begins to skew as it propagates through the shore, steepens

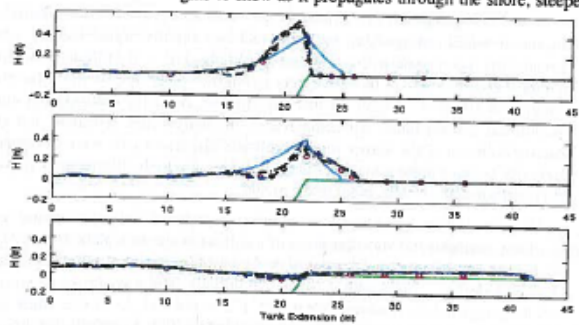

Fig. 5. Solitary wave over a dry reef, $A/d = 0.5$ and slope $1:5$, for NSWE (cyan), MS (blue) and Nowgu's equations (black), at times $t = 2.48, 3.83, 7.98$s. Circles denote measured data.

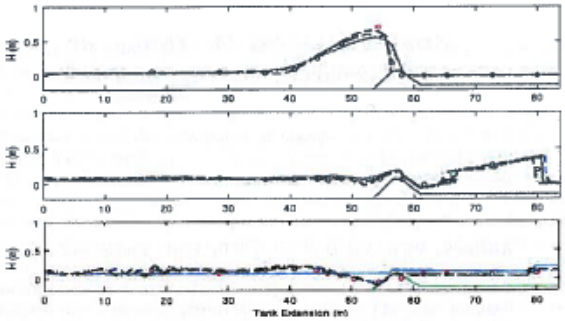

Fig. 6. Solitary wave over an exposed reef crest, $A/d = 0.3$ and $1:12$ slope, for NLSWE (cyan), MS (blue) and Nowgu's equations (black), at times $t = 6.82, 13.02, 48.94$s.

at the front but does not form a plunging breaker over the steep slope. From Fig. 5, it is obvious that NSWE can not reproduce the wave transformation until it reaches the shore. As the wave propagates on the shore the three models coincide due to the fact that the dispersive terms become zero and the Boussinesq models turns into shallow water equations. Fig. 6 shows the results from the second test case where the Boussinesq models have a exhibit a superior performance than the NSWE at later times.

References

[1] MADSEN, P.A., SÖRENSEN, O.R. 1992. A new form of the Boussinesq equations with improved linear dispersion characteristics. Patr 2. A slowing varying bathymetry. *Coastal Engineering*, **18**, 183–204.

[2] TONELLI, M. & PETTI, M., 2009. Hybrid finite-volume finite-difference scheme for 2DH improved Boussinesq equations *Coast. Eng.*, **56**, 609–620.

[3] NWOGU, O. 1993. An alternative form of the Boussinesq equations for nearshore wave propagation. *Journal of Waterway, Port, Coastal, and Ocsean Engineering*, **119**, 618–638.

[4] ROEBER, V., CHEUNG, K.F. & KOBAYASHI, M.H. 2010. Shock-capturing Boussinesq-type model for nearshore wave processes. *Coastal Engineering*, **57**, 407–423.

[5] WEI, G. & KIRBY, J.T 1995. A time-depented numerical code for extended Boussinesq equations. *Journal of Waterway, Port, Coastal, and Ocsean Engineering*, **120**, 251–261.

[6] SHIACH, J.B., MINGHAM, C.G. 2009. A temporally second-order acurate Godunov-type scheme for solving the extended Boussinesq equations. *Coastal Engineering*, **56**, 32–45.

[7] DELIS, A.I., KAZOLEA, M. & KAMPANIS, N.A. 2008. A robust high-resolution finite volume scheme for the simulation of long waves over complex domains *Int. J. Numer. Meth. Fluids*, **56**, 419–452.

[8] DELIS, A.I., NIKOLOS, I.K., & KAZOLEA, M. 2010. Performance and comparizon of cell-centered and node centered unstructured finite volume discretizations for shallow water free surface flows. *Archives of computational methods in engineering (ARCME)*, to appear.